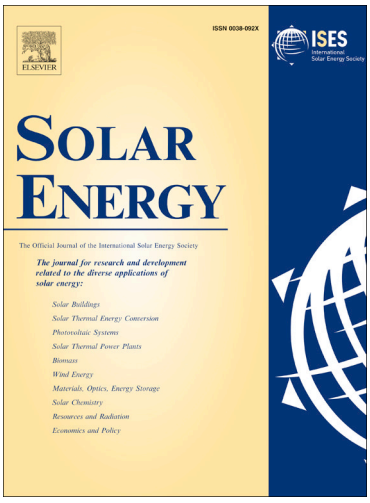

Seasonal caracterization of CIE standard sky types above Burgos, northwestern Spain

Andrés Suárez García, Diego Granados López, David González Peña, Montserrat Díez Mediavilla, Cristina Alonso Tristán

PII: S0038-092X(18)30373-6
DOI: https://doi.org/10.1016/j.solener.2018.04.028
Reference: SE 6764

To appear in: *Solar Energy*

Received Date: 16 January 2018
Revised Date: 11 April 2018
Accepted Date: 13 April 2018

Please cite this article as: Suárez García, A., Granados López, D., González Peña, D., Díez Mediavilla, M., Alonso Tristán, C., Seasonal caracterization of CIE standard sky types above Burgos, northwestern Spain, *Solar Energy* (2018), doi: https://doi.org/10.1016/j.solener.2018.04.028

SEASONAL CARACTERIZATION OF CIE STANDARD SKY TYPES ABOVE BURGOS, NORTHWESTERN SPAIN

Andrés Suárez García[1,2], Diego Granados López[2], David González Peña[2], Montserrat Díez Mediavilla[2], Cristina Alonso Tristán[2,*]

[1] Centro Universitario de la Defensa. Marín, Pontevedra, Spain. [2] Research Group Solar and Wind Feasibility Technologies (SWIFT). Electromechanical Engineering Department, Universidad de Burgos, Spain.

* Corresponding author: catristan@ubu.es

ABSTRACT

Outdoor daylight conditions in Burgos, Spain, are studied throughout a full year. The CIE standard sky type is selected in accordance with the lowest RMSD (Root Mean Square Deviation) following the comparison of both the theoretical and the experimental luminance distributions in the sky hemisphere. The selection is based on luminance distribution data, recorded every 30 min, from 145 patches of the sky hemisphere. The original criterion to determine the type of sky, the SSLD (the Standard Sky Luminance Distribution), is difficult to apply in certain places and at times when the solar elevation is higher than 35º. In consequence, two alternative procedures are used and compared in this study: the Tregenza method and the Normalization Rate (NR) introduced by Littlefair. The selection was taken from luminance distribution data of 145 patches of the sky hemisphere recorded between June 2016 and May 2017. The most frequent sky type observed in Burgos was V.5. (cloudless polluted with a broad solar corona), with a frequency of occurrence close to 20%. Notwithstanding that observation, the group of clear skies exhibited a higher frequency (in almost 50% of the cases under study, using both methods). The skies above Burgos were of an overcast sky type in less than 25% of cases, a situation with a higher likelihood in winter and in autumn, while in spring and summer the skies tended to be clear and cloud free. Both of the methodologies showed similar results in percentage terms and in confusion matrixes with almost insignificant differences when compared on a monthly, a seasonal, and an annual basis. Nevertheless, some mismatches were located in the highest solar elevation values.

KEYWORDS

CIE standard skies, luminance, daylight, Sky luminance distribution

NOMENCLATURE

γ, Z : Angle of elevation, angle from zenith	L_p : Luminance measured by the Sky-scanner of a sky patch (kcd/m^2)
α : Angle of azimuth	$L_{s,p}$: Luminance relative to the Zenith (dim)
α_s, γ_s : Solar azimuth, solar elevation	$L_{pr,st}$: Normalized luminance of a sky patch, corresponding to a standard sky (CIE)
n_p : Number of patches in band b	$L_{pr,sc}$**:** Normalized luminance of a sky patch, corresponding to an experimental measurement
b_p : Reference number of each band	E_h : Horizontal diffuse illuminance (kcd/m^2)
p : Reference number of a scanned sky patch	E_{hp}: Horizontal illuminance from sky patch p ($kcd/m^2 sr$)
	NR : Luminance normalization ratio (kcd/m^2)
	$L_{pred_{p,sc}}$: Normalized luminance (NR method) (kcd/m^2)

1. INTRODUCTION

Energy efficiency and sustainability are increasingly important issues in the field of architecture. Lighting often has the highest electrical consumption and cost in buildings with no air-conditioning systems and could account for over 40% of electricity costs in naturally ventilated offices. Daylighting is recognized as a key strategy in reducing energy consumption. The availability of natural light is highly recommendable for reasons of energy efficiency, visual comfort, and the physical and mental well-being of building occupants (Hwang and Jeong, 2011; Torrington and Tregenza, 2007).

Consequently, the recommendations of energy standards and green building rating systems strongly advise architects to incorporate daylighting strategies in their building designs (Aalto University School of Science and Technology, 2010). Architects and engineers need quantitative information on illumination levels and solar irradiance absorbed on surfaces at different inclinations for the incorporation of daylighting in the design of energy-efficient buildings and for suitable dimensioning of both the cooling and the heating systems. It requires an accurate estimation of the amount of available outdoor illuminance and of course the availability of daylight is mainly influenced by the levels and the patterns of luminance in the sky. To obtain sky luminance distribution, empirical models of homogeneous skies represents a low cost approach. Many of these methods(Li, 2010) are aimed at estimating daylight availability.

In 2003, the CIE categorization defined 15 standard sky types (Uetani et al., 2003). Sky types of the same category have the same well-defined sky luminance pattern. Once the sky types are identified, the basic solar irradiance and daylight illuminance on the surfaces of interest can be obtained through simple mathematical expressions (Li et al., 2013). The luminance distribution for each standard sky type can help arrive at accurate determinations of daylight illuminance (Kittler et al., 1997) . The classification includes five types of clear sky, five intermediate types, and five with cloud-cover. The distribution is characterized by continuous mathematical expressions to calculate smooth variations in luminance from the horizon to the zenith and in accordance with the angular distance from the sun. The general formula for defining the relative pattern of luminance for any sky type is a combination of a gradation function, dependent on two parameters, *a* and *b*, and the indicatrix function, which considers the scatter of luminance with regard to the direction of sunrays, which is modelled as a function of three adjustable parameters: *c*, *d,* and *e*. The gradation function modifies the luminance value between the horizon and the local zenith, assigning the highest luminance value to the zenith with cloudy skies and in reverse to clear skies, as shown

in Figure 1. The indicatrix function shows the dispersion in the atmosphere of sunlight, as represented in Figure 2. The maximum luminance appears near the solar position, decreasing rapidly with the distance to the sun. Each of the functions takes six different forms and the combination yields 36 sky types from which 15 were selected: five overcast, five partly cloudy, and five clear sky types, as shown in Table 1.

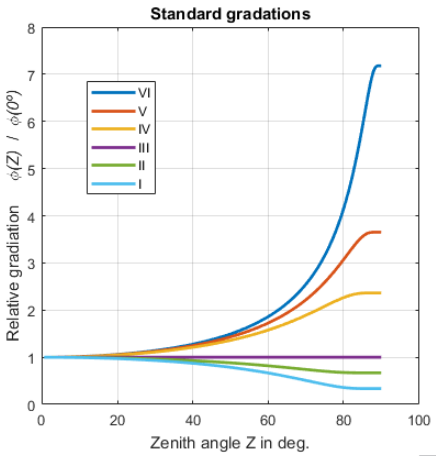

Figure 1. Relative gradation function

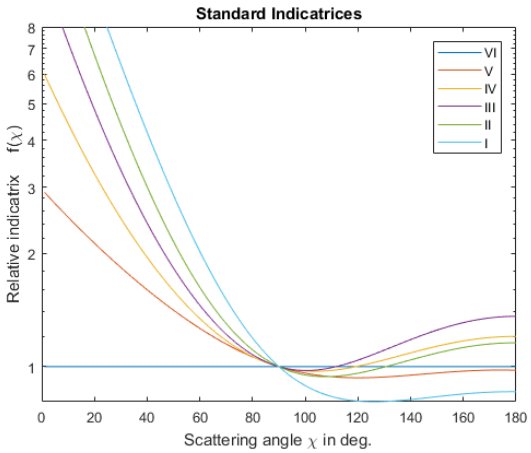

Figure 2. Relative indicatrix function.

Table 1. Parameters of CIE standard Sky types.

Type	a	b	c	d	e	Description
I.1	4.0	-0.70	0	-1.0	0.00	Overcast with a steep gradation and azimuthal uniformity
I.2	4.0	-0.70	2	-1.5	0.15	Overcast with a steep gradation and slight brightening toward sun
II.1	1.1	-0.80	0	-1.0	0.00	Overcast with a moderate gradation and azimuthal uniformity
II.2	1.1	-0.80	2	-1.5	0.15	Overcast with a moderate gradation and slight brightening toward sun
III.1	0.0	-1.00	0	-1.0	0.00	Overcast, foggy or cloudy, with overall uniformity
III.2	0.0	-1.00	2	-1.5	0.15	Partly cloudy with a uniform gradation and slight brightening toward sun
III.3	0.0	-1.00	5	-2.5	0.30	Partly cloudy with a uniform gradation and a brighter circumsolar effect
III.4	0.0	-1.00	10	-3.0	0.45	Partly cloudy, rather uniform with a clear solar corona
IV.2	-1.0	-0.55	2	-1.5	0.15	Partly cloudy with a shaded sun position
IV.3	-1.0	-0.55	5	-2.5	0.30	Partly cloudy with brighter circumsolar effect
IV.4	-1.0	-0.55	10	-3.0	0.45	White-blue sky with a clear solar corona
V.4	-1.0	-0.32	10	-3.0	0.45	Very clear / unturbid with a clear solar corona
V.5	-1.0	-0.32	16	-3.0	0.30	Cloudless polluted with a broader solar corona
VI.5	-1.0	-0.15	16	-3.0	0.30	Cloudless turbid with a broader solar corona
VI.6	-1.0	-0.15	24	-2.8	0.15	White-blue turbid sky with a wide solar corona effect

The sky type must first be known, in order to apply the CIE standard general sky type as per ISO 15469:2004 CIE S 011/E:2003 (2004) for determining luminance

distribution. The determination of the sky type at each location and time is a complex problem, due to the high fluctuation of the luminance magnitude and the influence of zenith luminance, that is determined with difficulty at low latitude locations. The original criterion to define the sky type, known as the SSLD method (Kittler et al., 1997) (Standard Sky Luminance Distribution), uses a theoretical assemblage of curves that represent the relation between the zenith luminance/diffuse illuminance (L_z/D_V) ratio and the solar elevation angle. These curves converge at solar elevation values higher than 35º, making it difficult to apply this method in certain areas and times when the solar elevation angle is higher than 35º, as can be seen in Figure 3. Several alternatives have been proposed involving the ratios of horizontal global illuminance and extra-terrestrial illuminance (G_v/E_V), horizontal sky diffuse illuminance and extra-terrestrial illuminance (D_v/E_V), the turbidity index, T_v (Li et al., 2014) and different climatic and atmospheric parameters (Kocifaj, 2011; Li et al., 2004). Machine learning algorithms and other progressive methods has also been used in the CIE standard sky classification (Li et al., 2010; Lima et al., 2016; Lou et al., 2017)

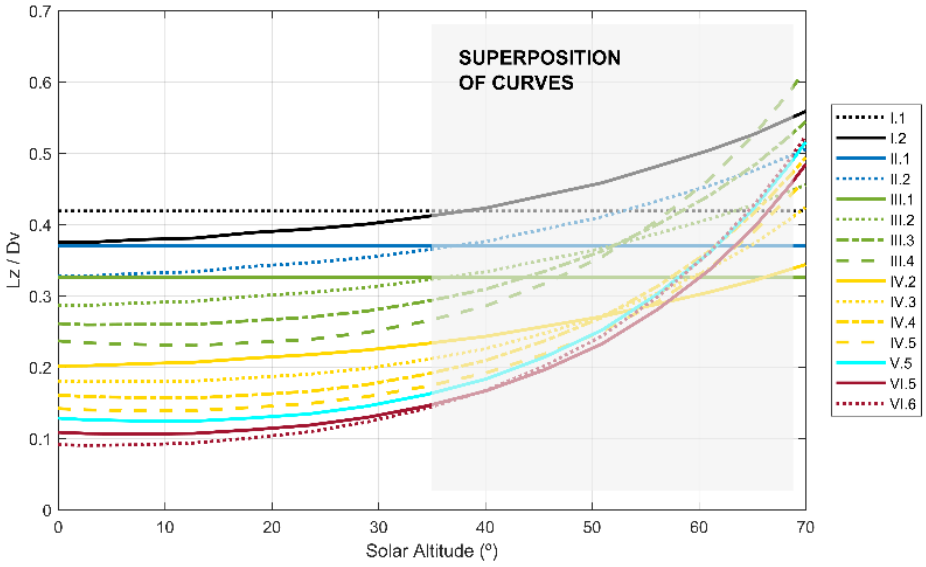

Figure 3. Graphical representation of the ratio zenith luminance/diffuse illuminance (L_z/D_V) vs solar altitude, where the convergence of the curves for values higher than 35º can be appreciated.

The application of the above-mentioned calculations to the successive sky conditions yields the statistical distribution of the General Sky types that best fit the sky luminance patterns at a given location and that consequently define the daylight climate of a given site. Notwithstanding its validity for calculating daylight availability, the empirical ISO/CIE model of homogeneous skies could be inaccurate when interpreting illuminances and irradiances on arbitrarily oriented surfaces under cloudy conditions (Kocifaj and Kómar, 2016) due to heterogeneity of cloud field.

Despite the high interest in these measurements, very few studies at only a handful of European (Bratislava, Athens, South England, Spain) and Asian (Honk Kong, Japan, Singapore) locations have been conducted to characterize the sky under the CIE standard (Markou et al., 2005; Markou et al., 2004; Torres et al., 2010a, b; Tregenza, 1999) (Chaiwiwatworakul and Chirarattananon, 2004; Li et al., 2003; Tregenza, 1999; Wittkopf et al., 2007) and over certain time periods (Torres et al., 2010a, b).

The main objective of this work is to define the daylight conditions in Burgos, northwestern Spain. A seasonal classification of the sky conditions was performed with a full year of data recordings. The SSLD method is not applicable to the location under study as the solar elevation of 35º is surpassed, especially in summer. Various procedures to circumvent this issue are proposed, using various methods of normalization, two of which were selected for comparison in this study. The first one is the widely accepted method proposed by Tregenza (Tregenza, 2004), consisting of a horizontal-based illuminance estimation. The second method, initially proposed by Littlefair (Littlefair, 1994a; Littlefair, 1994b), deals with the Normalization Ratio (NR) obtained by direct comparison between the CIE theoretical luminance and the experimental luminance levels; a method successfully applied to data recorded in Hong-Kong (Li et al., 2004; Li and Tang, 2008).

A Matlab code was developed for this purpose and a complete comparison of both methods is shown in a set of confusion matrixes. At the end, more than seven thousand samples were used. A complete year of measurement data was sufficient for a seasonal characterization of the skies over Burgos, referenced by the hour of the day. This study represents the first classification of this type in a Spanish city. Although both methodologies have been proposed for solar elevations higher than 35º, the NR approach is simpler and easier to compute than the Tregenza method. The results obtained by both methodologies in this study are perfectly comparable for the location under study and the solar elevation that is observed.

The study is organized as follows: “Experimental Section” describes the experimental facility used in this work, the meteorological features of the location under study and the experimental procedure. Section “CIE Standard Classification” summarizes the peculiarities of both methods applied for the CIE standard skies classification. The “Results” Section compares the sky classification according to both methodologies and presents the results in both graphical and numerical terms. Finally, the “Conclusions” Section summarizes the principal observations and the contributions of the study.

2. EXPERIMENTAL SECTION

CIE sky modelling and the application of the two methodologies was done using a code developed in Matlab.

2.1. Experimental facility

The experimental equipment used in this work is a commercial Sky-scanner model MS-321LR. The apparatus was installed on the roof of a building at Burgos University (42°21′04″N; 3°41′20″O; above mean sea level 856 m). Figure 4 shows the sky scanner equipment and its geographical location.

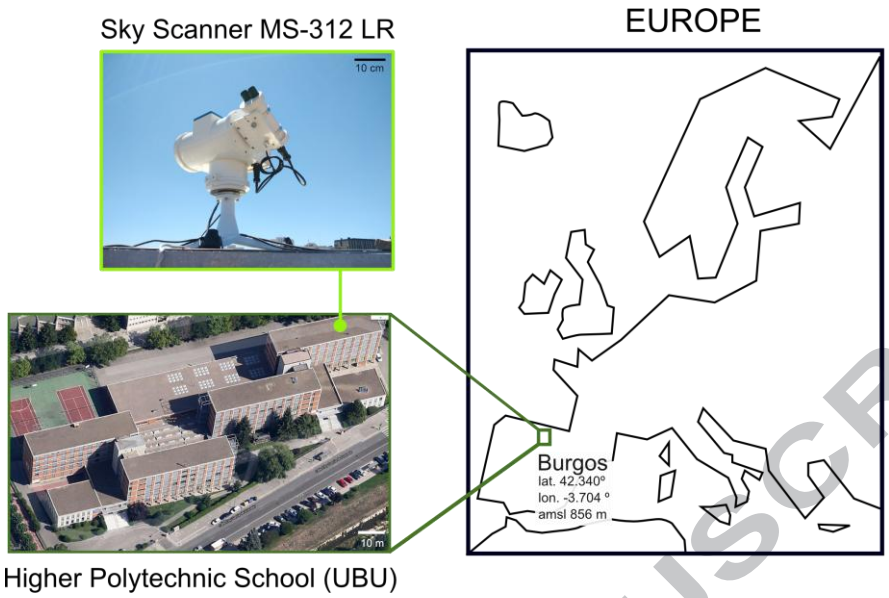

Figure 4. Location of the experimental apparatus on the roof of the Higher Polytechnic School building at the University of Burgos, Spain.

The period of time under analysis was in general warm and dry. Burgos has an average of 575 mm of precipitation and an average annual global irradiance of 1500 kWh/m^2, as can be seen in a Typical Meteorological Year (TMY) over the last twenty years, compiled by the Spanish State Meteorology Agency (AEMET) (ITACYL-AEMET, 2013). However, annual rainfall of 510 mm was recorded in the year under analysis (12% less than the TMY) and annual solar irradiance of 1650 kWh/m^2 (10% higher than the TMY) as shown in Figure 5. These data might bias the analysis, by giving the impression of a higher percentage of clear skies.

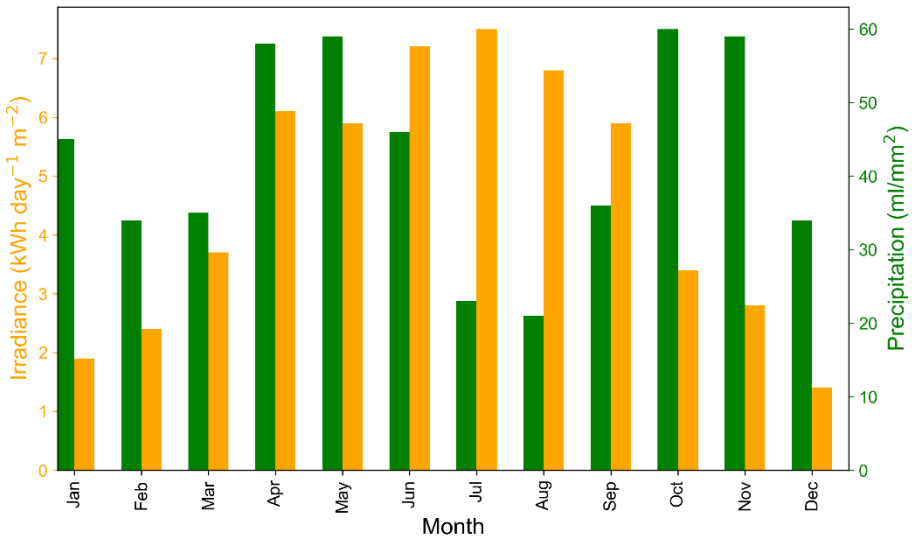

Figure 5. Global irradiance and precipitation in Burgos (MInisterio de Agricultura y Pesca)(June 2016 to May 2017)

According to the sky-scanner specifications, shown in Table 2, the sky is divided into 145 patches or sectors (*p*) that cover the whole dome. The sectors are grouped into eight bands, named b_p, and by their solar altitude $(\frac{\pi}{2} - Z)$, where Z is the zenith angle. Figure 6 shows the location of the sectors in the whole dome. A luminance measurement (kcd/m^2) of each patch is taken four times per hour. Half-hourly and hourly measurements taken between June 2016 and May 2017 were used for this study. Continuous scanning yielded luminance data corresponding to the 145 patches (see Fig. 6) recommended for the CIE in the Guide to Daylight Measurements, which were measured and registered. Likewise, the luminance corresponding to each of the commonly considered 15 standard sky types presented in Table 1 was calculated at the same time and for the same 145 patches. The standard sky type ascribed to each recorded moment showed the lowest RSMD (Root Mean Square Deviation) between the 145 normalized luminance values that were measured and calculated.

Table 2. Sky Scanner specifications

Model	MS-321LR Sky Scanner
Manufacturer	EKO Instruments

Dimensions (W x D x H)	430 mm x 380 mm x 440 mm
Mass	12.5 kg
Aperture	11 º
Illuminance	0 to 50 kcd/m^2
Radiance	0 to 300 W/m^2/sr
A/D Convertor	16 bit
Calibration Error	2 %

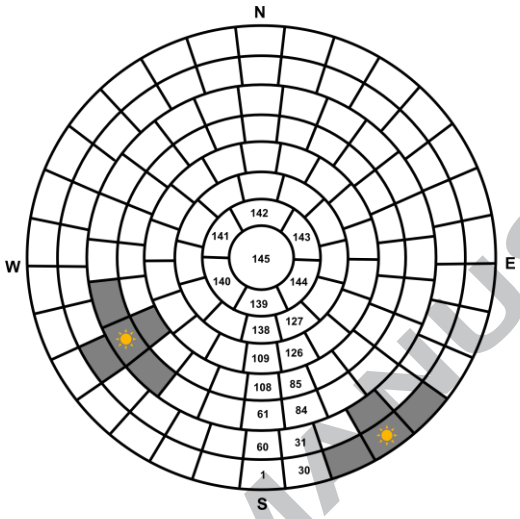

Figure 6. Sky divided into 145 sectors (p) grouped into 8 bands (b_p). The number of patches per band (n_b) is shown in the figure. Patches adjacent to the position of the sun are excluded from the luminance calculation.

2.2. Experimental procedure

Half-hourly and hourly measurements taken from June, 2016 to May 2017 were used in this study. The sky scanner is monthly adjusted to measure from the sunrise to the sunset. The first and last measurement of the day (solar elevation angle equal or lower than 5º) are discarded, as well measurements higher than 50 kcd/m^2 and lower than 0.1 kcd/m^2, following the specification of the equipment. Data pre-processing in Matlab code was performed, to avoid incorrect measurements. The number of available hourly data were classified by months, as shown in Figure 7. The abnormal number of available measurements in summer 2016, with the longest days of the year, is caused by modifications in the device.

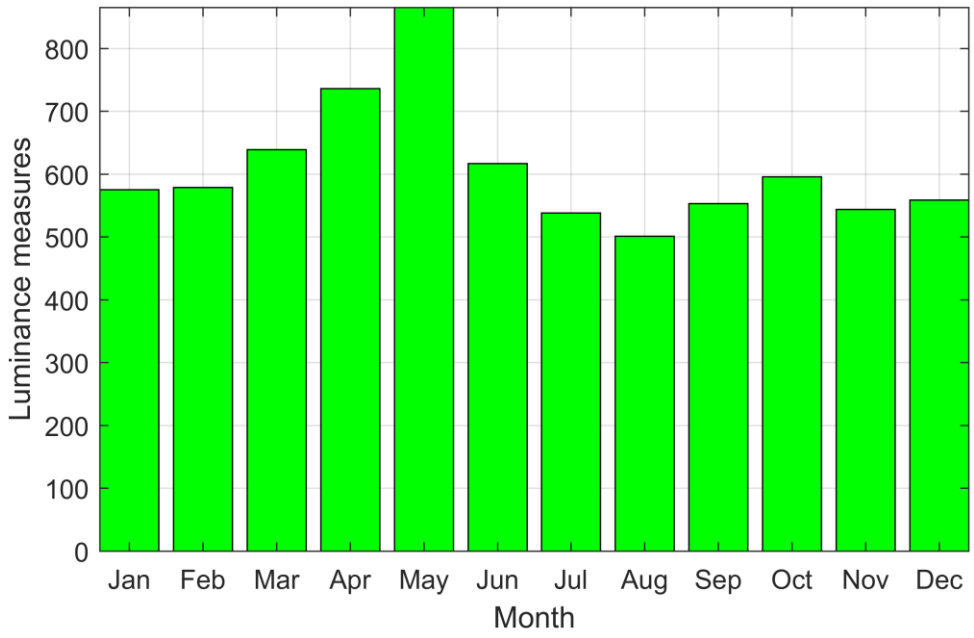

Figure 7. Number of available luminance measurements for the study.

3. CIE SKY CHARACTERIZATION

As mentioned in the introduction section, the two different methods applied in this study are both explained in this section.

3.1. The Tregenza Method.

The Tregenza method (Tregenza, 2004) calculates the horizontal diffuse illuminance, E_h (Eq. 1) in each scan. This value is the sum of the luminance from the different parts of the sky hemisphere. E_{hp}(Eq. 2) is the contribution of the measured luminance, L_p, coming from the patch p, to the horizontal diffuse illuminance. F_C is a correction factor that must be included because, in practice, the sum does not extend to the 145 patches. A few of them are discarded for the analysis due to two causes: a) according to the specifications of the instrument, luminance values lower than 0 kcd/m^2 or higher than 50 kcd/m^2 are outside the range of its measurements; and, b) patches close to the position of the sun should also be excluded, in order to avoid direct luminance. As can

be seen in Figure 6, the patches excluded for the calculation are those bordering the patch corresponding to the position of the sun.

$$E_h = F_c \sum_{p=1} E_{hp} \qquad \textit{Eq. 1.}$$

$$E_{hp} = \int_{\gamma_0}^{\gamma}\int_{\alpha_0}^{\alpha} L_p \, sin(\gamma)\, cos(\gamma)\, d\gamma d\alpha = \frac{L_p}{2}\left(\sin^2(\gamma) - \sin^2(\gamma_0)\right)(\alpha - \alpha_0) = L_P F_{g,p} \qquad \textit{Eq. 2,}$$

where, γ_0 is the sky patch´s basis, and γ is the top. $(\alpha - \alpha_0)$ is the azimuthal distance between patch's limits. $F_{g,p}$ is a geometrical factor characteristic to each patch. Eq. (3) is used for calculating the geometrical factor of a particular patch, taking into consideration the distribution of the 145 patches shown in Figure 6.

$$F_{g,p} = \frac{\pi}{n_p}\left\{sin^2\left(\frac{\pi\, b_p}{15}\right) - sin^2\left(\frac{\pi(\, b_p - 1)}{15}\right)\right\} for\ 1 \le b_p \le 7 \qquad \textit{Eq. 3,}$$

$$F_{g,p} = \pi\left\{1 - sin^2\left(\frac{\pi(\, b_p - 1)}{15}\right)\right\} \qquad for\ b_p = 8.$$

The correction factor, F_C, is calculated as:

$$F_C = \frac{\pi}{\sum_p F_{g,p}} \qquad \textit{Eq 4,}$$

where, the additions correspond only to the patches really considered for each scan. The normalized luminance distribution given for each patch, and for each sky type is given by:

$$L_{pr,sc} = \frac{L_p}{E_h} \qquad \textit{Eq. 5,}$$

where, $L_{pr,sc}$ is the previously normalized sky patch luminance, corresponding to one experimental measure. Additionally, the Tregenza method requires an estimate of the mean luminance of the Standard Sky type across each patch, *p*, of the scanning pattern, in order to make an accurate comparison with the measured values (Tregenza, 2004). So, we should take the mean of the luminances at the corners of the patch. The

mean luminance of each Standard Sky type of the first 144 elements, is the average luminance obtained in the four corners by each patch, given by the coordinates $Z = \left\{Z_p - \frac{\pi}{30}, Z_p + \frac{\pi}{30}\right\}$ and $\alpha = \left\{\alpha_p - \frac{\pi}{n_b}, \alpha_p + \frac{\pi}{n_b}\right\}$, where Z_p is the zenithal angle of each center patch, α_p is the azimuth angle, as shown in Figure 8, and n_b is the number of patches in the band (see Figure 6). Note that, for b_1, (patches from 1 to 30) only two corners are used in the average. The area around the zenith is split into six triangles, so the resulting average is the sum of each triangle calculated within its vertices.

$$L_{s145} = \frac{1}{9}\left\{3L_{sZenith} + \sum_{a=1}^{6} L_{sZenith\left[\frac{\pi}{30}, \frac{a\pi}{3} - \frac{\pi}{6}\right]}\right\} \qquad \textit{Eq. 6.}$$

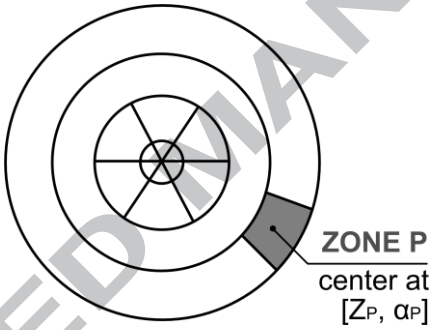

Figure 8. Scheme of the average done to obtain the luminance of each patch.

It is also possible to obtain normalized theoretical measurements, by using equation 2 to calculate the corresponding horizontal illuminance. Starting from that point, if the luminance of each patch is divided by the previously calculated horizontal illuminance, $L_{pr,st}$, fifteen sets of average normalized luminance are obtained, one for each type of standard sky. Finally, each standard sky type will be compared with the previously measured and normalized ($L_{pr,st}$) experimental sky type.

The RMSE is obtained by comparing the measured patch luminance with standard sky type luminance, excluding the empty patches from the sum under the square root. The type of sky is obtained by picking out the lowest $RMS_{sc,\ st}$ from the fifteen possible types.

$$rms_{sc,st} = \sqrt{\frac{\sum(L_{pr,sc} - L_{pr,st})^2}{n}} \qquad \textit{Eq 7.}$$

$L_{pr,st}$ is the normalized luminance of a sky patch, corresponding to a (CIE) standard sky, $L_{pr,sc}$ is the normalized luminance of a sky patch, corresponding to an experimental measurement; N is the number of measurements, excluding the empty patches. Finally, sc refers to an experimental type and st is the particular standard sky type that is tested.

3.2. The Littlefair Normalization Ratio (NR)

Luminance can be normalized according to the Normalization Ratio introduced by Littlefair (Littlefair, 1994a); Littlefair (1994b)) and described by (Li and Tang, 2008). This method was developed to be applied at locations where high solar altitudes dominate. The luminance normalization ratio (NR) is given by:

$$NR = \frac{\sum L_p \cos(\gamma) \sin(\gamma) d\gamma \, d\alpha}{\sum L_{s,p} \cos(\gamma) \sin(\gamma) d\gamma \, d\alpha} \qquad \text{Eq. 8,}$$

where, L_p is the luminance (kcd/m^2) measured by the Sky scanner, excluding luminance higher than 50 kcd/m^2 and lower than 0.1 kcd/m^2 and direct luminance values; $L_{s,p}$ is the predicted sky path luminance in a relative form given by CIE (Eq. 2); γ is the angle of elevation of the sky point above the horizon (radians) and α is the azimuth of a sky patch (radians).

Finally, the predicted sky luminance value is calculated by multiplying the relative theoretical luminance by the Zenith and the normalization ratio, as follows:

$$L_{pred_{p,sc}} = L_{s,p} \, NR \qquad \textit{Eq. 9.}$$

After normalizing the luminance, the sky type is chosen from the best fit with the 15 CIE Standard skies, in accordance with the lowest $rRMSE_{sc}$ value:

$$rRMSE_{sc} = \sqrt{\frac{1}{n}\sum_i \left(\frac{L_{pred,sc} - L_p}{L_p}\right)^2} \qquad \textit{Eq. 10.}$$

N is the number of non-empty readings, *p* refers to the path of the sky or the number *i*, $L_{pred,p,sc}$ is the normalized luminance obtained using the NR factor and L_p is the luminance measured in kcd/m^2 by the Sky scanner.

4. RESULTS

The classifications of the two previously described normalization procedures are compared in this study. In view of the differences, the overall annual comparison was disaggregated into hourly periods. First, an annual comparison of the classifications of both algorithms was completed; second, the CIE and cloudiness types were grouped by seasons (summer, autumn, winter and spring) to identify the times of year with larger differences. The hourly relative differences of both models were estimated, by selecting the months of the season with the biggest discrepancies. Finally, all of the cloudiness models were compared in a confusion matrix. All of those analyses contribute to the characterization of the differences between both methods.

4.1. Seasonal classification of skies in Burgos

Figure 9 shows the relative frequency of each sky type over the period of study, calculated using both the Tregenza and the NR method. As can be seen in both figures, all sky types of the CIE classification, shown in Table 1, can be found in Burgos, from overcast to very clear. The lowest frequency is for type I.2, corresponding to Overcast with the steep gradation and slight brightening toward the sun, and the highest frequency is for type V.5. (Cloudless polluted with a broader solar corona). Both methods present very few differences and are almost equivalent in the II.2, IV.3 and V.5 sky types, as shown in Figure 9. The biggest differences in the classification

were found in types IV.2 and VI.5. These results were grouped into different time intervals, in order to find a pattern that produces the aforementioned gap.

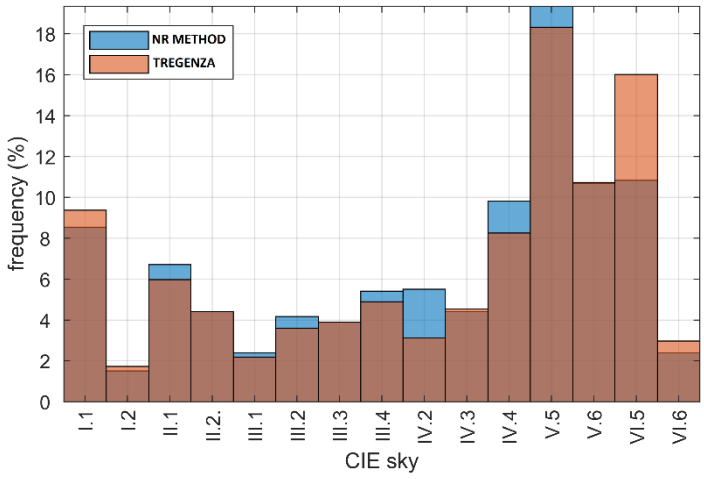

Figure 9. Comparative characterizations of the skies over Burgos

One characteristic of Burgos is that all types of CIE skies classification can be found throughout the year. This fact can be observed in the monthly classification of the results of both methods shown in Figures 10 (a) and 10 (b). Sky types I.1, I.2, V.5. and V.6 are predominant in winter (almost 10% frequency each). clear types of sky (IV.4, V.5.V.6 and VI.5) prevail in spring and summer time. In summer, type IV.2, corresponding to a partly cloudy sky is also frequent. Autumn is a clear sky season too.

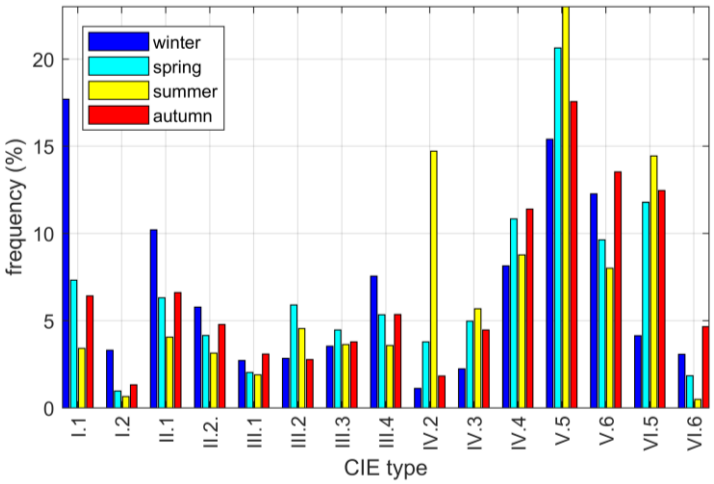

(a)

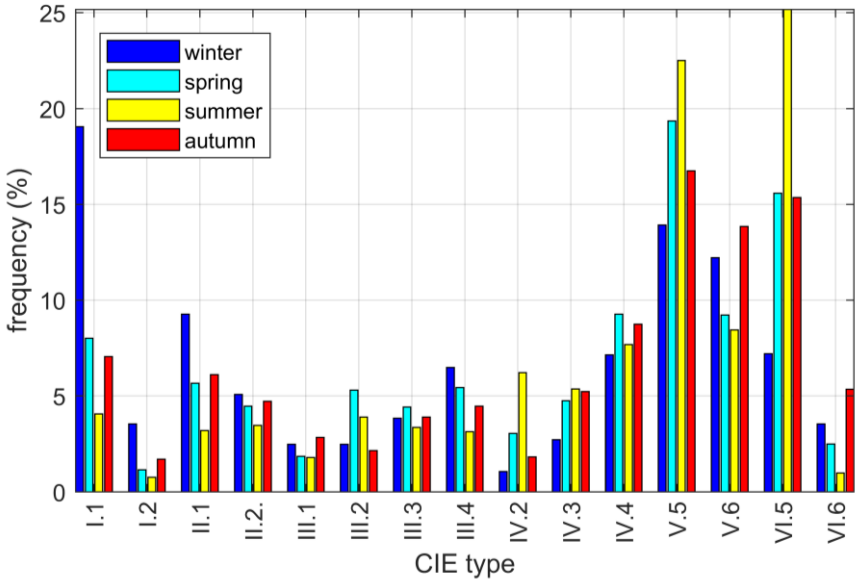

(b)

Figure 10. Seasonal CIE sky types histogram over Burgos calculated using the NR method (a) and the Tregenza Method (b)

Grouping the CIE types by seasons clearly profiles the switch between the IV.2 and VI.5 sky types. As can be seen in Figure 10a, the NR method classifies 15% of the skies in summer as IV.2 and almost 22% as VI.5. In contrast, the Tregenza method

classified 25% of the skies as VI.5, in the same season, as shown in Figure 10b. It also labelled 6% of the recorded skies as IV.2. Sky type VI.5. appeared in 23% of cases when using the Tregenza method. It is evident that the mismatch is limited to 9% of all records. The differences between both methods in the other seasons of the year are insignificant.

The values of E_h would coincide for different types of sky in specific positions of the sun in the hours of sunrise and / or sunset (Kocifaj, 2012). In these cases, this magnitude, which is what the Tregenza method uses to perform the classification (Eq. 3), can lead to an inadequate result. The NR method uses L_p, a magnitude that differs more in these sky conditions.

4.2. Cloudiness classification

Cloudiness labelling was done with the CIE sky types: I.1 to III.1 were classified as cloudy, III.2 to IV.3 as partially cloudy, and IV.4 to VI.6 as clear skies. These three categories, represented in Figure 11, reflect the characteristically clear skies that it is predominant in Burgos. According to both methods, a clear sky type was present every month in almost 50% of cases, as can be seen in Figures 12 (a) and 12 (b). An overcast sky type was observed in Burgos in less than 25% of cases, a situation more probably in winter and autumn, while in spring and summer the skies were mainly clear.

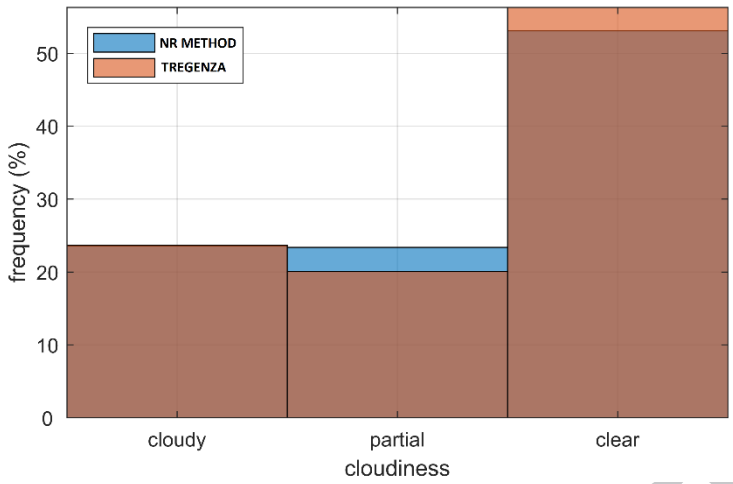

Figure 11. Comparative study of cloudiness classifications in Burgos.

The differences in the cloudiness classifications of the methods are clearly visible in the months of June, July and August. The NR method (Figure 12a) classified a lower percentage of clear skies than the Tregenza method (Figure 12b) in the three aforementioned months. The percentages of the skies classified as cloudy, partially cloudy, and clear, over the remaining months are almost identical.

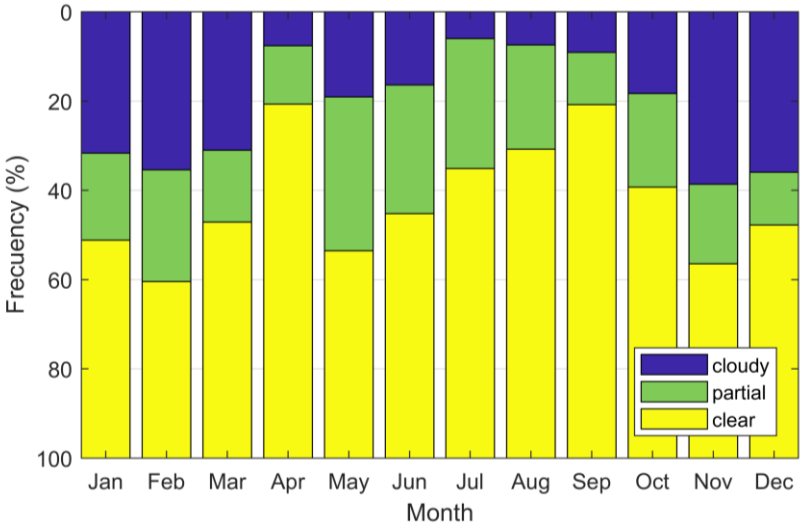

(a)

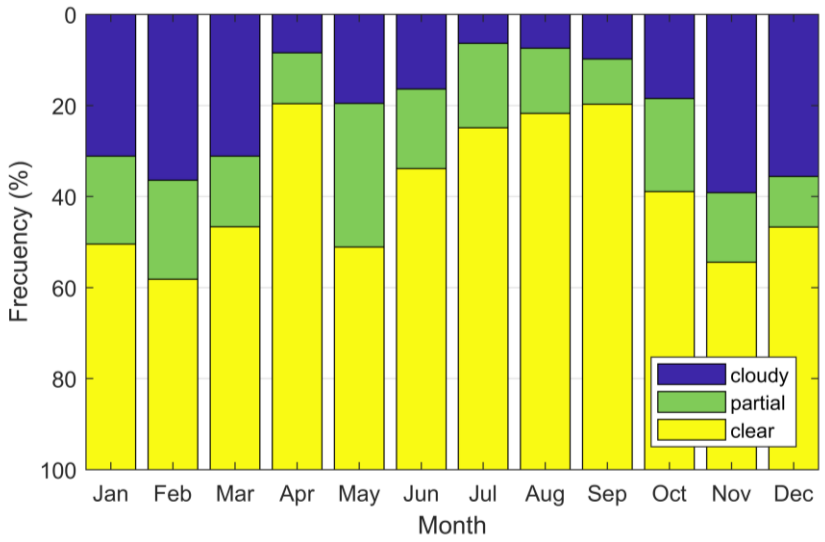

(b)

Figure 12. Burgos sky cloudiness grouped by months using NR method (a) and Tregenza method (b)

4.3. Analysis of summer time by daytime hour

The CIE relative differences in the classifications grouped by daytime hours during the summer months was prepared to examine the differences in greater detail. The results are shown in Figure 13. There are several forms of estimating the relative difference between both magnitudes (Bennett and Briggs, 2008). In the present work, neither algorithm can be considered superior, because there are no qualitative differences between either one. Eq. 11 was used to estimate the relative difference between the frequencies grouped by daytime hours.

$$d_r = \frac{|x-y|}{\max(|x|,|y|)} \qquad \textit{Eq. 11.}$$

It may be easily noted that the main divergence between CIE sky types IV.2 and VI.5 are at midday hours. There are also other points where the relative difference is above 50%. However, their weight in the global percentages is irrelevant, as Figure 13 shows. In summary, the main differences between the Tregenza and the NR methods are at

highest solar altitudes of the year that take place in the central hours of the day during summer.

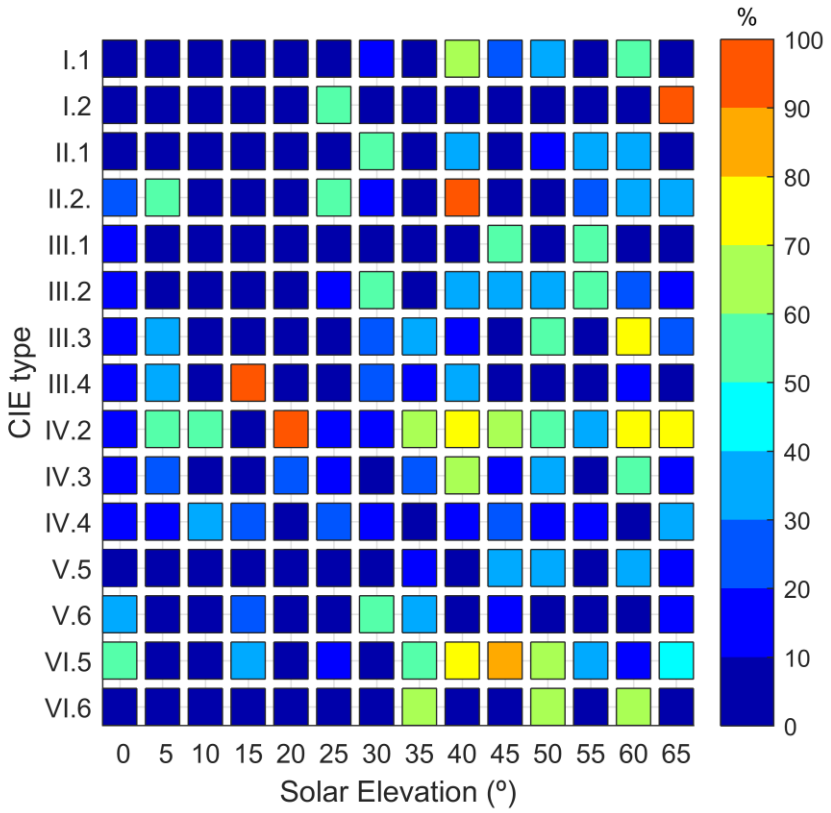

Figure 13. Relative difference, d_r, calculated using Eq. 11, between the NR and the Tregenza sky classifications, for the summer months.

4.4. Confusion matrix of Tregenza and NR Methods

The results of both the Tregenza and the NR methods were compared in a confusion matrix; an indicatrix of the matches between two series of values. The confusion matrix is shown in Figure 14. In this case, the cloudiness classifications of the two methods are compared step by step. Each square of the table shows the number of coincidences and their corresponding percentages. The upper-left 3x3 matrix corresponds to the raw comparison, coding the cells either in green, if Tregenza and NR agree, or in red, if otherwise. The gray cells are the percentages that count the total cases in each row or column. Finally, the blueish cell to the lower-left shows the extent

of global matching. As it can be seen, the global coincidences for the cloudiness classification amount to 94.3 %.

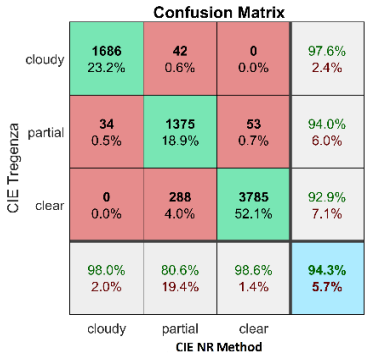

Figure 14. Confusion matrix comparing the Tregenza and the NR cloudiness classifications.

4.5. Comparison between the goodness indicators of each method.

As previously explained, both methods used in this study define the type of sky based on a goodness indicator, the RMSE (Root Mean Square Error), but the definition of this statistical indicator is different for each method. While the NR method uses the luminance normalized ratio NR defined by eq. 10, Tregenza uses the horizontal diffuse illuminance to normalize the values. The RMSE values calculated for both methods are therefore not comparable values.

One solution to this issue would be a new definition of the relative *rRMSE* coupled with another widely used statistical indicator, the relative Mean Bias Error *(rMBE).* Both indices are defined in equations 12 and 13. The rMBE provides information on the grade of dispersion relating to the center of the distribution and is a good dispersion indicator of the model versus the reality (Bennett and Briggs, 2008). The comparison

was done using the theoretical CIE Luminance that refers to the Zenith, without normalization, $L_{sp,st}$, and the experimental Luminance, $L_{sp,}$, calculated using the above method:

$$rMBE_{sc} = \frac{1}{N}\sum_p \left(\frac{L_{sp,}-L_{sp,st}}{L_{sp,}}\right) \quad \textit{Eq. 12.}$$

$$rRMSE_{sc} = \sqrt{\frac{1}{N}\sum_p \left(\frac{L_{sp}-L_{sp,st}}{L_{sp}}\right)^2} \quad \textit{Eq. 13.}$$

N is the number of measurements, excluding the empty patches. Table 3 shows the results obtained using this new criterion. As can be seen, the unification of the normalization criterion permits the numerical comparison of both methods. Both methodologies, as mentioned throughout the study, are applicable to the area under study and both statistical indicators yielded similar results, offering low MBE values at high solar elevations.

Table 3. Statistical indicators RMSE and MBE, calculated using eq. 12 and 13

	$\alpha \in (0, \frac{\pi}{2})$		$\alpha < 35º$		$\alpha > 35º$	
	rRMSE	*rMBE*	*rRMSE*	*rMBE*	*rRMSE*	*rMBE*
Tregenza method	36.7 %	14.1%	34.9%	13.1%	40.1%	16.0%
NR method	36.0%	13.3%	33.4%	11.4%	40.8%	17.0%

5. CONCLUSIONS

Two different methodologies, Tregenza and NR, to define the CIE standard sky types in the skies over Burgos, Spain, have been applied and compared. Both methods are recommended for use in areas where the latitude is higher than 35º, which is the case of Burgos. The best-fitting sky types and their frequency of occurrence have been studied over a complete year. The low value of the RMSE index shows that both methods tend to get a very acceptable agreement between predictions and measured

values, so both methods can be used with high confidence at the latitude of Burgos. However, this study shows that this confidence will decrease at the highest solar altitudes. In addition, this study supports the fact that, despite the crucial aspect of normalized luminance, some effective and very different methods exist. The NR method uses a statistical parameter (NR) while the Tregenza method uses the horizontal illuminance, although the results are realistic, accurate, and very similar. As the confusion matrix has shown, the matches between both models were very good, so it comes as no surprise that the frequency distribution was likewise very similar. The smooth differences in the frequency distribution of the sky type found can be explained by the consideration of homogenous skies inherent of the CIE standard classification. The luminance of a partly cloudy sky can vary over a wide range even if the cloud fraction is stable for a long time and CIE standard classification does not account for such variability.

The aim of this research work has been to determine the frequency distribution of each Sky type, so as to obtain quantitative information on the levels of illumination and solar radiation on surfaces. Both methods confirm that the most frequent sky type observed in Burgos is V.5. (cloudless polluted with a broad solar corona), with a frequency of occurrence close to 20%. Nevertheless, the group of clear skies has a higher frequency (in almost 50% of the cases under study for both methods). The skies over Burgos are of an overcast type in less than 25% of cases, a situation with a greater likelihood in both winter and autumn, while in spring and summer the sky is predominantly clear. The summer skies over Burgos are very clear and the winter is quite cloudy. Although those results show clear skies over Burgos during the year that is under study, additional years of measurement will be needed to arrive at a clear picture of global behavior that excludes years of drought and excessive rainfall.

The generalization of the results will be given the more cases are performed by the scientific community. It can be expected seasonal behavior in the measurements and

results obtained. Hence, it would be necessary a multi-year analysis in order to avoid the aforementioned bias. However, as it was said, given the amount of samples analyzed, the differences detected cannot be deprecated. Not only the development of new sky models is important in the field of science that concerns us, but also, their comparison and the discern of their strengths in order to use them in an optimum way.

ACKNOWLEDGEMENTS

The authors gratefully acknowledge the financial support provided by the Regional Government of Castilla y León (Ref. BU034U16), under European Regional Development Fund, and the Spanish Ministry of Economy, Industry and Competitiveness, under the I+D+i State Programme Challenges for the Society (Ref. ENE-2014-54601-R). David González Peña would also like to thank the Junta de Castilla-León for economic support (PIRTU Program, ORDEN EDU/301/2015). Finally, Andrés Suárez García extends his thanks to the International Excellence Triangular-E^3 for financing his stay under the Centrally Managed Programme of the Ministry of Education, Culture & Sports (BOE 295, 10th December 2015).

BIBLIOGRAPHY

Aalto University School of Science and Technology, I.E.A., 2010. Guidebook on Energy Efficient Electric Lighting for Buildings. Raisio, IEA publications.

Bennett, J.O., Briggs, W.L., 2008. Using and Understanding Mathematics: A Quantitative Reasoning Approach.

Chaiwiwatworakul, P., Chirarattananon, S., 2004. Distribution of sky luminance in tropical climate. Proceedings of the Joint International Conference on Sustainable Energy and Environment, Hua Hin, 530-537

Hwang, T., Jeong, T.K., 2011. Effects of indoor lighting on occupants' visual comfort and eye health in a green building. Indoor and Built Environment 20(1), 75-90

ITACYL-AEMET, 2013. Atlas Agroclimático de Castilla y León http://atlas.itacyl.es. (Accessed January, 2017.

Kittler, R., Perez, R., Darula, S., 1997. A new generation of sky standards. In: Proceedings of the Eighth European lighting conference , Amsterdam, pp. 359–373., 359-373

Kocifaj, M., 2011. CIE standard sky model with reduced number of scaling parameters. Sol. Energy 85(3), 553-559

Kocifaj, M., Kómar, L., 2016. Modeling diffuse irradiance under arbitrary and homogeneous skies: Comparison and validation. Appl. Energy 166, 117-127

Li, D.H.W., 2010. A review of daylight illuminance determinations and energy implications. Appl. Energy 87(7), 2109-2118

Li, D.H.W., Chau, N.T.C., Wan, K.K.W., 2013. Predicting daylight illuminance and solar irradiance on vertical surfaces based on classified standard skies. Energy 53, 252-258

Li, D.H.W., Chau, T.C., Wan, K.K.W., 2014. A review of the CIE general sky classification approaches. Renewable Sustainable Energy Rev 31, 563-574

Li, D.H.W., Lau, C.C.S., Lam, J.C., 2003. A study of 15 sky luminance patterns against hong kong data. Architectural Science Review 46(1), 61-68

Li, D.H.W., Lau, C.C.S., Lam, J.C., 2004. Standard skies classification using common climatic parameters. J Sol Energy Eng Trans ASME 126(3), 957-964

Li, D.H.W., Tang, H.L., 2008. Standard skies classification in Hong Kong. J. Atmos. Sol.-Terr. Phys. 70(8), 1222-1230

Li, D.H.W., Tang, H.L., Lee, E.W.M., Muneer, T., 2010. Classification of CIE standard skies using probabilistic neural networks. Int. J. Climatol. 30(2), 305-315

Lima, F.J.L., Martins, F.R., Pereira, E.B., Lorenz, E., Heinemann, D., 2016. Forecast for surface solar irradiance at the Brazilian Northeastern region using NWP model and artificial neural networks. Renew. Energy 87, 807-818

Littlefair, P.J., 1994a. A comparison of sky luminance models with measured data from Garston, United Kingdom. Sol. Energy 53(4), 315-322

Littlefair, P.J., 1994b. The luminance distributions of clear and quasi-clear skies, Proceedings of the CIBSE National Lighting Conference, Cambridge, UK. pp. 267-283.

Lou, S., Li, D.H.W., Lam, J.C., 2017. CIE Standard Sky classification by accessible climatic indices. Renew. Energy 113, 347-356

Markou, M.T., Kambezidis, H.D., Bartzokas, A., Katsoulis, B.D., Muneer, T., 2005. Sky type classification in Central England during winter. Energy 30(9 SPEC. ISS.), 1667-1674

Markou, M.T., Kambezidis, H.D., Katsoulis, B.D., Muneer, T., Bartzokas, A., 2004. Sky type classification in South England during the winter period. Building Research Journal 52(1), 19-30

MInisterio de Agricultura y Pesca, A.y.M.A., SIAR: Sistema de Información Agroclimática para el Regadío. http://www.mapa.es/siar/Informacion.asp (Accessed January, 2018.

Torres, J.L., de Blas, M., García, A., Gracia, A., de Francisco, A., 2010a. Sky luminance distribution in Pamplona (Spain) during the summer period. J. Atmos. Sol.-Terr. Phys. 72(5-6), 382-388

Torres, J.L., de Blas, M., García, A., Gracia, A., de Francisco, A., 2010b. Sky luminance distribution in the North of Iberian Peninsula during winter. J. Atmos. Sol.-Terr. Phys. 72(16), 1147-1154

Torrington, J.M., Tregenza, P.R., 2007. Lighting for people with dementia. Lighting Research & Technology 39(1), 81-97

Tregenza, P.R., 1999. Standard skies for maritime climates. Lighting Research & Technology 31(3), 97-106

Tregenza, P.R., 2004. Analysing sky luminance scans to obtain frequency distributions of CIE Standard General Skies. Lighting Research & Technology 36(4), 271-279

Uetani, Y., Aydinli, S., Joukoff, A., Kendrick, J., Kittler, R., Koga, Y., 2003. Spatial distribution of daylight-CIE standard general sky. Vienna, Austria

Wittkopf, S.K., Soon, L.K., Ng, E.Y.Y., 2007. Analysing sky luminance scans and predicting frequent sky patterns in Singapore. Light Res Technol 39(1), 31-51

Highlights

- Outdoor daylight conditions in Burgos, Spain, are studied throughout a full year.
- The CIE standard sky type has been selected.
- Two alternative procedures to the SSLD have been applied and compared.
- The most frequent sky type observed in Burgos was V.5.
- The group of clear skies exhibited a frequency nearly of 50% of the studied cases.